ACS APPLIED MATERIALS & INTERFACES

RESEARCH ARTICLE

www.acsami.org

High Performance Dye-Sensitized Solar Cells with Alkylpyridinium Iodide Salts in Electrolytes

Semina Jeon,[†,‡] Yimhyun Jo,[§] Kang-Jin Kim,[‡] Yongseok Jun,[*,§] and Chi-Hwan Han[*,†]

[†]Photovoltaic Research Center, Korea Institute of Energy Research, 71-2, Jangdong, Yuseong, Daejeon 305-343, Republic of Korea

[‡]Department of Chemistry, Korea University, Seoul, 136-713, Republic of Korea

[§]Interdisciplinary School of Green Energy, UNIST, Ulsan, 689-798, Republic of Korea

ABSTRACT: Pyridinium iodide salts, which are competitive to the conventional imidazolium iodide salts, have been used for dye-sensitized solar cells as iodide sources and ionic conductivities. Pyridinium iodide series are easy to prepare and less expensive than the imidazolium series salts. In this research, quite comparable efficiencies were obtained from electrolytes with pyridinium iodide salts. For the experiments, pyridinium salts with a few different alkyl chains are applied. When a pyridinium head is modified to picolinium, which has a methyl group on the pyridinium head, a noticeable V_{oc} drop has been observed. However, the length of the alkyl chains on the pyridinium head does not affect V_{oc} effectively. The odd-numbered alkyl chains showed slightly lower V_{oc} compared to that of the even-numbered alkyl chains. Finally, the performances of the cells with pyridinium salts are compared to those of the conventional cells with imidazolium salts.

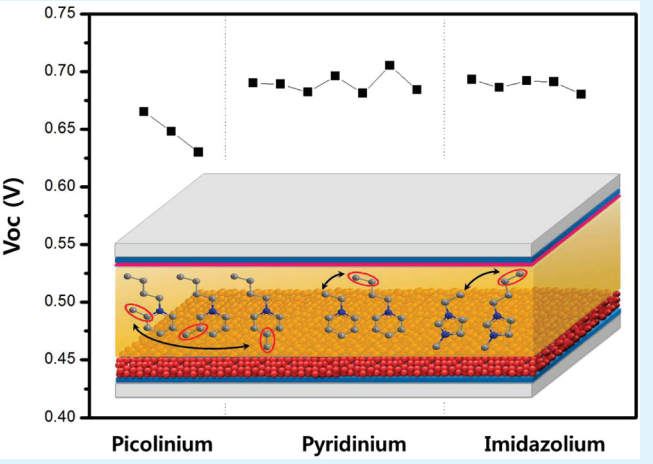

KEYWORDS: dye-sensitized solar cell, pyridinium salts, electrolyte

INTRODUCTION

Since the application of mesoporous nanocrystalline thin films to dye-sensitized solar cells was introduced, there has been growing interest because of its high conversion efficiency with possible low production cost.[1−5] The common dye-sensitized solar cell (DSSC) consists of a working electrode of nanocrystalline TiO_2 with dyes,[6−12] a counter electrode usually with Pt,[13,14] and an electrolyte system with I^-/I_3^- between the electrodes.[4,5]

From the early stage of DSSC research, the composition of electrolytes includes simple ionic salts such as LiI, KI, and alkylammonium iodide in acetonitrile-based solvent.[15−20] When LiI and KI are used in an electrolyte, small cations (Li^+, K^+) travel through dyes and adsorb on the TiO_2 surface. This lowers the Fermi level of the TiO_2 working electrode by a positive charge, which results in a voltage drop. Note that the maximum voltage (V_{oc}, open circuit voltage) is determined by the potential difference between the Fermi level of the TiO_2 electrode and the reduction/oxidation potential of the redox species in an electrolyte. Once the Fermi level is lowered by the cations, the driving force to transfer electrons from dyes to the conduction band of TiO_2 can increase, and barriers for the electron flow can be lowered. Therefore, a current increase is observed. For this reason, voltage increases and current drops are very common trade-off phenomena in the DSSC system. To relieve the small cationic effect on the voltage drop, the electrolyte composition for ionic salts has been modified to alkylimidazolium iodide. If the size of the cation increases, less cations can reach and occupy the TiO_2 surface; therefore, a relatively higher voltage can be expected.[21−24]

Because common alkylimidazolium salts and ionic liquid show very good thermal stability in a wide range of voltages (near 4 V) in electrochemistry, they are well studied and broadly applied to many systems, such as Li^+ ion secondary batteries, fuel cells, and DSSCs.[25,26] Alkylimidazolium salts with halides, which are necessary in a DSSC system, show lower thermal stability than alkylimidazolium salts with other anions. The decomposition temperature for alkylimidazolium halide to imidazole and alkyl halide is near 270 °C, while imidazolium salts and ionic liquid with other anions such as trifluoromethylsulfonyl anion show a higher decomposition temperature near 500 °C. Once decomposition starts, the conductivity of the electrolyte will drastically decrease because the consequent products are alkyl halides, which are not ionic salts.[25,26]

Witkamp described long-term stabilities of imidazolium and pyridinium ionic compounds by considering decomposition mechanism and temperature. The prediction has been achieved by quantum chemical calculation at the B3LYP level. According to the calculation, the decomposition mechanism is the second-order

Received: November 11, 2010
Accepted: January 4, 2011
Published: January 26, 2011

substitution reaction (SN2), and pyridinium ionic liquids show lower decomposition temperatures than imidazolium ionic liquids by up to 100 °C.[26] The expected decomposition temperature for pyridinium iodide salts is near 170 °C.

Because most ionic compounds, including ionic liquids, are developed for endurable applications at high temperature in applications such as batteries and fuel cells, pyridinium compounds have obtained less attention. However, DSSCs do not require good stability at a temperature higher than 170 °C while running. Therefore, salts and ionic liquids based on the pyridinium cation might be applicable for the electrolyte systems in DSSCs. Currently, most of the pyridine derivatives are only considered as additives in an electrolyte for increasing the Fermi level of TiO_2 working electrodes. Pyridine derivatives are very resistant to oxidation and transparent in a wide range of spectra. These basic characteristics, with a low cost for preparation, might be useful for DSSC applications.

In this paper, we synthesized a series of alkylpyridinium iodide and applied them to DSSCs successfully. We observed the cation effect on the TiO_2 nanoparticle surface with dependence on the alkyl chain length with an odd or even number of carbons. In addition, the results of pyridinium salts have been compared with ones of the conventional imidazolium salts.

EXPERIMENTAL SECTION

Materials. The ionic liquids, except 1-alkylpyridinium iodides, were purchased from Iolitec. Purity of the purchased ionic liquids was ≥98%. The 1-alkylpyridinium iodides (R = ethyl, butyl, hexyl, heptyl, octyl, nonyl, and dodecyl) were synthesized by reflux of pyridine and *n*-alkyliodide (R = ethyl, butyl, hexyl, heptyl, octyl, nonyl, and dodecyl) in 1:1 molar ratio at 100 °C for 3 h and then washed with anhydrous ethanol to remove unreacted starting materials at least three times. The washed products were vacuum-dried at 80 °C for 2 h. The syntheses were confirmed with NMR and infrared spectroscopy.

Ionic Conductivity Measurement. Ionic conductivity of the electrolytes was determined by the impedance method. Electrochemical impedance spectroscopy (EIS) measurement was carried out with IM6 (Zahner). The frequency range in EIS measurement was 0.05−105 Hz. The magnitude of the alternative signal was 10 mV, and the applied bias is 0.0 V. Conductivity of a liquid was measured from the obtained solution resistance or bulk resistance, R_s, using the following formula (eq 1)

$$\sigma = l/R_s \times A \quad (1)$$

where σ is the conductivity ($\Omega^{-1}cm^{-1}$ or S/cm), l is the distance between two electrodes, which is the thickness of the solution (cm), A is the electrode area (cm^2), and R_s is the bulk resistance (Ω).

Preparation of TiO_2 Photoelectrode and Ru(II) Dye Coating. The TiO_2 paste (Ti-nano oxide D, Solaronix) was deposited on the conducting glass with a fluorine-doped stannic oxide layer (FTO, TEC 8/2.3 mm, 8 Ω/□, Pilkington) by using a screen-printing method. The resulting layer was calcined for 2 h at 470 °C in a muffle furnace. This process was repeated three times or until a thickness of 15 μm was obtained. The area of the prepared porous TiO_2 electrode was 25 mm^2 (5 mm × 5 mm). Dye absorption was carried out by dipping the TiO_2 electrode in a 4×10^{-4} M *t*-butanol/acetonitrile (Merck, 1:1) solution of the standard ruthenium dye, N719 (Solaronix), for 48 h at 25 °C. The photoelectrode was then washed, dried, and immediately used to measure the performance of the solar cell.

Fabrication of Dye-Sensitized Solar Cell. Transparent counter electrodes were prepared by placing a few drops of 10 mM hydrogen hexachloroplatinate (IV) hydrate (99.9%, Aldrich) and 2-propanol solution on drilled FTO glass. After calcining at 450 °C for 2 h, the counter electrodes were assembled with dye-absorbed TiO_2 photoelectrodes. The two electrodes were separated by 25 μm Surlyn and sealed by heating. The internal space was filled with electrolyte, and the drilled hole was sealed with Surlyn and coverglass.

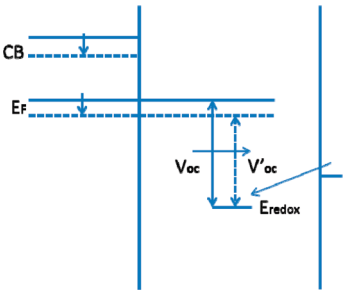

Figure 1. Energy diagram for dye-sensitized solar cells. When cations lower the Fermi level of TiO_2, an open circuit voltage drop ($V_{oc} \rightarrow V'_{oc}$) is expected, as shown in this diagram.

Photovoltaic Characterization. The photoelectrochemical properties of the prepared DSSCs were measured by using a computer-controlled digital source meter (potentiostat/galvanostat model 273A, EG & G) and a solar simulator (AM 1.5, 100 mW/cm^2, Oriel) as a light source. Photovoltaic performance has been characterized by V_{oc}, J_{sc}, fill factor (FF), and overall efficiency by a *J-V* curve. V_{oc} is the electrical potential between photoanodes and cathodes of solar cells with extremely large external loads. J_{sc} is the measured current when the circuit between the photoanode and cathode has a least-resistance connection. FF is the ratio of maximum power performance to its ideal maximum power by V_{oc} and J_{sc}. η can be defined as ($V_{oc} \times J_{sc} \times$ FF) divided by P_s, where P_s is the intensity of the incident light.

RESULTS AND DISCUSSION

Usually, V_{oc} changes in DSSC are explained by TiO_2 Fermi level movement, where the energy level of a redox couple in an electrolyte is fixed. When cations adsorb on the TiO_2 surface, they affect the surface charge, and then the conduction band and the Fermi level of TiO_2 shifts to a lower direction. This shift results in a voltage drop as shown in Figure 1. In this experiment set, Li^+ ions are the main cations that affect the TiO_2 Fermi level because pyridinium cations (>1.0 nm) are much larger than Li^+ ions (0.18 nm). Pyridinium cations are also available on the surface, and they occupy a much larger area than Li^+. Therefore, bulkier cations on the TiO_2 surface will relieve lowering of the conduction band edge by Li^+ ions. To utilize this cation size effect, many researchers have tried imidazolium cations instead of Li^+. This effect has been observed even in alkali metal ion size changes such as Li^+, Na^+, K^+, and Cs^+.[18,27,28]

There is another common factor that determines the Fermi level of a TiO_2 surface. Additives such as tertiary-butyl pyridine (TBP, 0.7 nm) are believed to adsorb on the TiO_2 surface, where dyes are not coated, and then Li^+ ion's approach can be blocked. Therefore, a negative shift of TiO_2 bands occurs, thus the V_{oc} increases. In addition, it is believed that TBP on a TiO_2 surface reduces recombination through back transfer to an electrolyte.[22] However, a certain amount of Li^+ is desired because lowering the Fermi level of TiO_2 can drive an easier transfer of electrons from dyes to TiO_2. This trade-off effect is commonly used when a newly changed DSSC system needs optimized.

On the basis of the explanation, voltage changes can be mainly discussed with a level of concentration of cations at the

Table 1. Ionic Salts for the Experiment and Their Abbreviations

Ionic salts	Abbreviation	Chemical Structure
1-Butyl-α-picolinium iodide	α-C4**PiI**	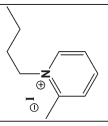
1-Butyl-β-picolinium iodide	β-C4**PiI**	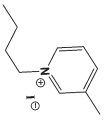
1-Butyl-γ- picolinium iodide	γ -C4**PiI**	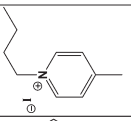
1-Alkylpyridinium iodide	C*n***PI**	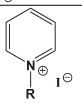 R=ethyl (C2**PI**), butyl(C4**PI**), etc.
1-Alkyl-3-methylimidazolium iodide	C*n***ImI**	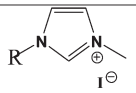 R=ethyl (C2**ImI**), butyl(C4**ImI**), etc.

TiO_2 surface and additives such as TBP. When more cations with less TBP are available at the unit surface, a lower V_{oc} is expected.

Pyridinium Salt and Picolinium Salts. In order to consider pyridinium salts, we prepared simple 1-butylpyridinium iodide (C4**PI**, C4 = butyl) derivatives. When a methyl group is added to the α-, *β*-, or *γ*- position of pyridinium salts, they are called picolinium salts (α-, *β*-, *γ*-C4**PiI**). Detail structures and full names are listed in Table 1. When they are prepared in the solvent, their ionic conductivities are almost the same, from 2.45 to 2.58 mS/cm. This means their dissociation properties in the solvent are very similar to each other, and no noticeable differences in the *J-V* characteristics are expected from the ionic conductivities. Figure 2 shows *J-V* characteristics of the cells with each electrolyte. Although the electrolyte with α-C4**PI** ($E_{\alpha\text{-C4PiI}}$) shows the best efficiency among the picolinium salts, it did not reach the efficiency of the cell with E_{C4PI}. In the picolinium series, the V_{oc} ranges from 0.665 to 0.630 V, which is much lower than the value for a cell with E_{C4PI}, 0.689 V. As will be discussed later, all the systems with pyridinium salts (E_{CnPI}) show V_{oc} values of near 0.69 V. The low voltage for the picolinium series might be due to cation bulkiness. Because of the methyl group on the α-, *β*-, and *γ*- positions of pyridine, picolinium sizes are larger in width. The high randomness in ionic structure in picolinium cations due to the methyl group hinders their lateral assembly on the TiO_2 surface. This could result in more Li^+ ions on possible cation sites, less TBP on the surface, or both. Either one can show V_{oc} lowering. When the adsorption of Li^+ cations is more effective, a voltage drop occurs with a current density increase. However, we observed only a voltage drop without a noticeable current density decrease. This could be due to picolinium's steric hindrance to the TiO_2 surface. Because TBP does not effectively approach the TiO_2 surface, the increased electrons by V_{oc} lowering could be scattered to the electrolyte through the surface state, which is not covered by TBP.

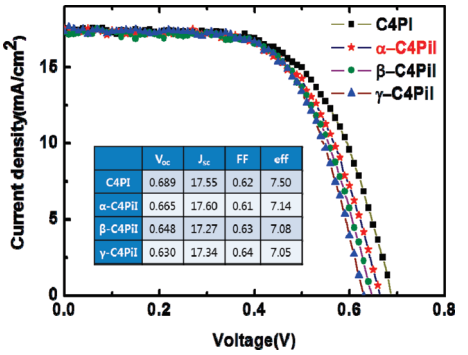

Figure 2. *J-V* characteristics of the cells with each electrolyte: C4PI (■), α-C4**PiI** (red star), *β*-C4**PiI** (green circle), and *γ*-C4**PiI** (blue triangle). Units for V_{oc} and J_{sc} in the inset are V and mA/cm^2, respectively.

Because V_{oc} values are 0.665, 0.648, and 0.630 V for α-, *β*-, and *γ*-picolinium salts, respectively, bulkiness of the head part affect the voltage changes more effectively. As discussed in the next section, these noticeable V_{oc} changes are not observed in pyridinium salts with a variation of normal alkyl chain length.

Chain Length Dependence for Pyridinium Salts. To understand the dependence of the molecular structure of cations in salts, we prepared a few salts with different alkyl chain lengths of pyridinium cations. To prevent any possible effect from side chains, all the cations have only normal alkyl chains from 2 to 9 carbons (Table 1). Depending on the number of alkyl carbons, pyridinium salts were abbreviated as C*n***PI**, where *n* is the number of carbons. For example, C6PI means 1-hexylpyridinium iodide. The ionic conductivities of the salts in the solvent vary from 2.41 to 2.08 mS/cm, slightly decreasing when the chain length increases. Figure 3 shows V_{oc} characteristics for the cells with electrolytes containing C*n***PI**, where *n* is from 2 to 9. For all the pyridinium salts, their V_{oc} values are greater than ones for the

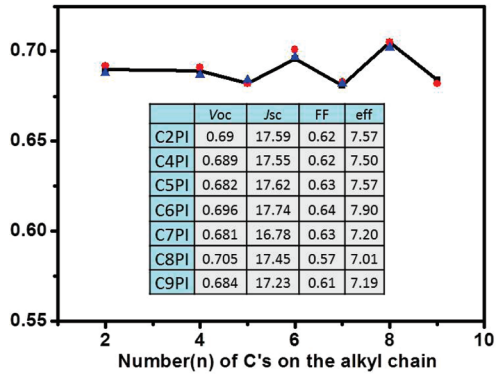

	Voc	Jsc	FF	eff
C2PI	0.69	17.59	0.62	7.57
C4PI	0.689	17.55	0.62	7.50
C5PI	0.682	17.62	0.63	7.57
C6PI	0.696	17.74	0.64	7.90
C7PI	0.681	16.78	0.63	7.20
C8PI	0.705	17.45	0.57	7.01
C9PI	0.684	17.23	0.61	7.19

Figure 3. *J-V* characteristics of the cells with each electrolyte; C*n***PI**. Units for V_{oc} and J_{sc} in the inset are V and mA/cm^2, respectively. (Each experimental set is symbolized with a different figure).

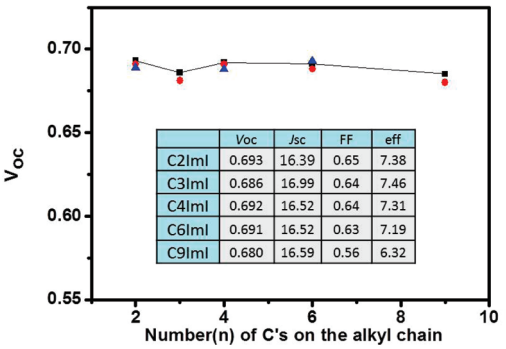

	Voc	Jsc	FF	eff
C2Iml	0.693	16.39	0.65	7.38
C3Iml	0.686	16.99	0.64	7.46
C4Iml	0.692	16.52	0.64	7.31
C6Iml	0.691	16.52	0.63	7.19
C9Iml	0.680	16.59	0.56	6.32

Figure 4. *J-V* characteristics of the cells with each electrolyte; C*n***ImI**. Units for V_{oc} and J_{sc} in the inset are V and mA/cm^2, respectively. (Each experimental set is symbolized with a different figure).

previous picolinium salts, and no noticeable trend is observed. Although the average value for each chain length is increasing, this difference is only about 5 to 10 mV. Note that picolinium cations showed a V_{oc} drop up to 60 mV. When it comes to the structure of molecule, alkyl chain tails can stay behind the pyridine head. Once they reach the TiO_2 surface, pyridinium cations can laterally assemble on the surface like self-assembled monolayers (SAMs). Therefore, voltage changes, depending on alkyl chain length in pyridinium series, is very limited.

Although chain length does not affect this phenomenon effectively, there is one interesting observation for the chain length dependence. When the alkyl chain lengthens from E_{C2PI} to E_{C8PI}, V_{oc} values remained almost the same, or slightly increased. However, V_{oc} values with E_{C5PI}, E_{C7PI}, and E_{C9PI} are noticeably lower than the chain length trend, and all of them have odd number of carbons in the alkyl chains.

Even-numbered or odd-numbered alkyl chain dependence is well-known in SAM studies on solid substrates. For example, siloxane monolayers on a silicon oxide surface or thiol monolayers on a metal (Au, Ag, or Pt) surface show different packing structures, depending on even or odd numbered alkyl chain length.[29,30] Because no research has been achieved about SAMs of alkyl pyridines on a TiO_2 surface, it is very difficult to give a direct explanation for their geometry on the TiO_2 surface. Especially, charged pyridine could show a different tendency from possible pyridine-related SAMs. Depending on the pyridine head configuration on a TiO_2 surface, their alkyl tail could show different packing structures. However, the mechanism could be quite related to the even- and odd-numbered alkyl chain effect. For instance, cations with even-numbered alkyl chains have lower packing densities on the TiO_2 surface due to its tail configuration; therefore, less positive charge densities are expected on the unit area. As a consequence, higher voltage can be expected. Of course, there could be other factors such as Li^+ penetration, TBP adsorption availability, and dye configuration. This complexity makes it hard to suggest a clear explanation in detail at this moment.

In addition, there are two possibilities for pyridinium cations on the surface. They can either lie down on the surface or be laterally packed to make SAMs. On the basis of the V_{oc} results, they may prefer lateral assemblies on the surface to lying down. If they lie down on the surface, a longer chain length will cover a larger area, which must increase or at least change V_{oc} values. However, the V_{oc} values are changing only less than 10 mV. This value is much smaller than 60 mV, which was observed in the picolinium cations series. Note that picolinium cations have bulkier cations, which are not preferable for lateral packing.

Comparison with Imidazolium Salts. Finally, the cells with $E_{\text{pyridinium salts}}$ are compared with the cells with $E_{\text{imidazolium salts}}$. For the comparison, we prepared 3-methylimidazolium iodide series with similar lengths. The number of carbons in the main axis has been changed from 2 to 9. Each was shortened to C*n***ImI**. For example, (**1-ethyl**)-3-methylimidazolium iodide is abbreviated to C2**Im**I. Although we observed similar effects to the pyridinium salts case, such as V_{oc} changes on length and a even and odd number of carbons, the tendency is much weaker and unclear as shown in Figure 4. This might be due to the methyl group on the 3-nitrogen in imidazolium, which may mainly disturb packing of imidazolium cations on the TiO_2 surface.

The ionic conductivities for solution with imidazolium salts are slightly lower than the ones for solutions with pyridinium salts. The solution with the imidazolium series showed the ionic conductivities from 1.91 to 2.29 mS/cm, while the values for pyridinium salts are from 2.08 to 2.41 mS/cm. The cells with $E_{\text{pyridiniums salts}}$ generally show higher current densities, and this might be related to the ionic conductivities.

For the direct comparison, the best cells among each series were chosen. The best performance with $E_{\text{imidazolium salts}}$ was obtained from the cells with E_{C3ImI}, which is 7.46% with 0.686 V (V_{oc}), 16.99 mA/cm^2 (J_{sc}), and 0.64 (FF). The best cell with E_{C6PI} shows a higher performance than the best cell with E_{C3ImI}. The cell with E_{C6PI} showed better *J-V* characteristics in all terms, 7.92% with 0.696 V (V_{oc}), 17.74 mA/cm^2 (J_{sc}), and 0.641 (FF). Cells with $E_{\text{pyridinium salts}}$ are quite competitive to the conventional cells with $E_{\text{imidazolium salts}}$.

Figure 5 shows the UV absorption spectra with IPCE spectra for the cells, which shows the best efficiencies among each series. For a comparison, UV spectra for C6ImI are added. We observed the higher quantum efficiency from the cell with E_{C6PI} in the wide range from 460 to 800 nm, while the quantum efficiencies are almost the same in the range of shorter wavelengths. This might be imparted because C6PI absorbs more incident light than C3ImI at the short wavelength range. When the absorption of incident light is weak after 500 nm, the quantum efficiencies of the cell with C6PI are noticeably higher. The absorption trend of C6PI is compared with C6ImI, which is one of the common ionic salts for current DSSCs. Although absorption coefficients for C6PI are greater than those for C6ImI over all the range, the cell efficiencies are quite comparable. This visible region absorption

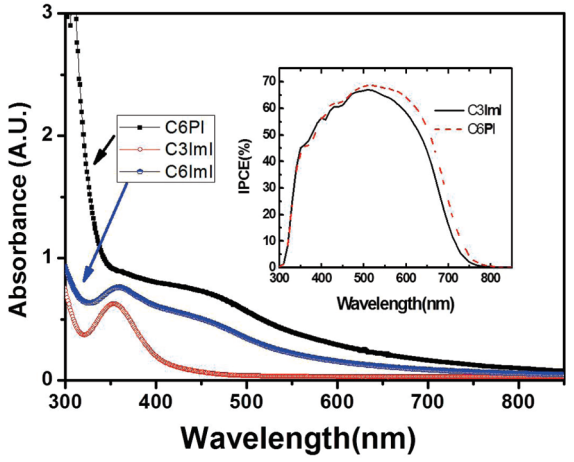

Figure 5. UV−vis spectroscopy selected pyridinium and imidazolium salts. The inset is the IPCE data for the cells with E_{C3ImI} and E_{C6PI}, which are the best cells among each series.

could be avoided by varying alkyl chains. The absorption spectra for C2PI, C4PI, and picolinium series do not have any noticeable peaks at the region of longer wavelengths than 400 nm.

CONCLUSION

Pyridinium salts have been used in DSSC electrolyte systems as iodide source and ionic conductivity, and quite comparable results to the conventional imidazolium salts are obtained in this study. For the experiments, pyridinium salts containing cations with different alkyl chains are applied. Possible reasons are suggested for V_{oc} changes, depending on structures of pyridinium cations. When the pyridinium head is modified to picolinium, which has a methyl group on the pyridinium head, a drastic V_{oc} drop has been observed. However, the length of alkyl chains does not affect V_{oc} effectively. In addition, odd-numbered alkyl chains showed slightly lower V_{oc} compared to even-numbered alkyl chains. A possible reason for the observation has been also discussed. Finally, the performance of the cells with $E_{pyridinium}$ salts are compared to the conventional cells with $E_{imidazolium}$ salts. We believe that this inexpensive and easy way of preparation of pyridinium salts might give advantages for commercialization of DSSCs.

AUTHOR INFORMATION

Corresponding Author

*Phone: +82 52 217 2919 (Y.J.), +82 42 860 3061 (C.-H.H.). Fax: +82 52 217 2909 (Y.J.), +82 42 861 6224 (C.-H.H.). E-mail: yjun@unist.ac.kr (Y.J.), hanchi@kier.re.kr (C.-H.H.).

ACKNOWLEDGMENT

This research was supported by the National Research Foundation of Korea (NRF) funded by the Korean Government (MEST) (Converging Research Center Program 2010K001086, 2010-0011167, and NRF-2009-C1AAA001-2009-0092950).

REFERENCES

(1) Shin, K.; Jun, Y.; Moon, J. H.; Park, J. H. *ACS Appl. Mater. Interfaces* **2009**, *2*, 288–291.
(2) O'Regan, B.; Grätzel, M. *Nature* **1991**, *353*, 737–740.
(3) Lee, H. S.; Bae, S. H.; Jo, Y.; Kim, K. J.; Jun, Y.; Han, C. H. *Electrochim. Acta* **2010**, *55*, 7159–7165.
(4) Hagfeldt, A.; Grätzel, M. *Acc. Chem. Res.* **2000**, *33*, 269–277.
(5) Grätzel, M. *J. Photochem. Photobiol., C* **2003**, *4*, 145–153.
(6) Lv, X.; Wang, F.; Li, Y. *ACS Appl. Mater. Interfaces* **2010**, *2*, 1980–1986.
(7) Schmidt-Mende, L.; Bach, U.; Humphry-Baker, R.; Horiuchi, T.; Miura, H.; Ito, S.; Uchida, S.; Grätzel, M. *Adv. Mater.* **2005**, *17*, 813–815.
(8) Ahmad, S.; Yum, J. H.; Butt, H. J.; Nazeeruddin, M. K.; Grätzel, M. *ChemPhysChem* **2010**, *11*, 2814–2819.
(9) Gao, F.; Wang, Y.; Shi, D.; Zhang, J.; Wang, M.; Jing, X.; Humphry-Baker, R.; Wang, P.; Zakeeruddin, S. M.; Grätzel, M. *J. Am. Chem. Soc.* **2008**, *130*, 10720–10728.
(10) Kuang, D.; Ito, S.; Wenger, B.; Klein, C.; Moser, J. E.; Humphry-Baker, R.; Zakeeruddin, S. M.; Grätzel, M. *J. Am. Chem. Soc.* **2006**, *128*, 4146–4154.
(11) Wang, P.; Klein, C.; Humphry-Baker, R.; Zakeeruddin, S. M.; Grätzel, M. *J. Am. Chem. Soc.* **2005**, *127*, 808–809.
(12) Lee, H. J.; Leventis, H. C.; Haque, S. A.; Torres, T.; Grätzel, M.; Nazeeruddin, M. K. *J. Power Sources* **2011**, *196*, 596–599.
(13) Papageorgiou, N. *Coord. Chem. Rev.* **2004**, *248*, 1421–1446.
(14) Imoto, K.; Takahashi, K.; Yamaguchi, T.; Komura, T.; Nakamura, J. I.; Murata, K. *Sol. Energy Mater. Sol. Cells* **2003**, *79*, 459–469.
(15) Hagfeldt, A.; Didriksson, B.; Palmqvist, T.; Lindström, H.; Södergren, S.; Rensmo, H.; Lindquist, S. E. *Sol. Energy Mater. Sol. Cells* **1994**, *31*, 481–488.
(16) Kay, A.; Grätzel, M. *Sol. Energy Mater. Sol. Cells* **1996**, *44*, 99–117.
(17) Knödler, R.; Sopka, J.; Harbach, F.; Grünling, H. W. *Sol. Energy Mater. Sol. Cells* **1993**, *30*, 277–281.
(18) Liu, Y.; Hagfeldt, A.; Xiao, X. R.; Lindquist, S. E. *Sol. Energy Mater. Sol. Cells* **1998**, *55*, 267–281.
(19) Smestad, G. *Sol. Energy Mater. Sol. Cells* **1994**, *32*, 273–288.
(20) Smestad, G.; Bignozzi, C.; Argazzi, R. *Sol. Energy Mater. Sol. Cells* **1994**, *32*, 259–272.
(21) Kopidakis, N.; Neale, N. R.; Frank, A. J. *J. Phys. Chem. B* **2006**, *110*, 12485–12489.
(22) Kusama, H.; Orita, H.; Sugihara, H. *Langmuir* **2008**, *24*, 4411–4419.
(23) Son, K. M.; Kang, M. G.; Vittal, R.; Lee, J.; Kim, K. J. *J. Appl. Electrochem.* **2008**, *38*, 1647–1652.
(24) Watson, D. F.; Meyer, G. J. *Coord. Chem. Rev.* **2004**, *248*, 1391–1406.
(25) Kroon, M. C.; Buijs, W.; Peters, C. J.; Witkamp, G. J. *Green Chem.* **2006**, *8*, 241–245.
(26) Kroon, M. C.; Buijs, W.; Peters, C. J.; Witkamp, G. J. *Thermochim. Acta* **2007**, *465*, 40–47.
(27) Fredin, K.; Nissfolk, J.; Boschloo, G.; Hagfeldt, A. *J. Electroanal. Chem.* **2007**, *609*, 55–60.
(28) Salvador, P.; Hidalgo, M. G.; Zaban, A.; Bisquert, J. *J. Phys. Chem. B* **2005**, *109*, 15915–15926.
(29) Colorado, R., Jr; Villazana, R. J.; Lee, T. R. *Langmuir* **1998**, *14*, 6337–6340.
(30) Tao, F.; Bernasek, S. L. *Chem. Rev.* **2007**, *107*, 1408–1453.